# New Procedure to Determine Neutrino Mass

M. H. Sidky

Department of Engineering, Mathematics and Physics, Faculty of Engineering, Cairo University, Egypt
sidkym@yahoo.com

**Abstract:** The neutrino mass $m_\nu$ is determined as well as the probability of occurrence of the 0νββ decay mode $P^{0\nu}$. The lower and upper limits of $m_\nu$ and $P^{0\nu}$.form an operating region. In this the work the double beta decay emitters $^{82}Se$ , $^{100}Mo$ , $^{116}Cd$ , $^{128}Te$ , $^{130}Te$ , $^{136}Xe$ and pn-QRPA , pn-RQRPA , full-RQRPA and SQRPA techniques with small and large basis of Hilbert space have been used to construct 48 operating regions. The best one belongs to $^{130}Te$ and pn-RQRPA technique with small basis of Hilbert space. This corresponds to $m_\nu \pm \delta m_\nu = 0.269 \pm 0.0216$ eV . This result agrees with a previous determinations and improve the relative uncertainty $\delta m_\nu / m_\nu$ from 12.5% to 8%.

[M. H. Sidky. **New Procedure to Determine Neutrino Mass.** *J Am Sci* 2012;8(12):1274-1279]. (ISSN: 1545-1003). http://www.jofamericanscience.org. 172

**Keywords:** Procedure; Determine; Neutrino Mass

## 1. Introduction:

Nuclear physics can contribute to the solution of questions concerning the nature of neutrinos by investigation of neutrinoless double beta decay (0νββ) decay mode. The hypothetical neutrinoless (0νββ) decay mode can only occur for massive Majorana neutrinos [1]. This decay may be mediated by the exchange of a Majorana neutrino or by other new particles [2]. The recent discovery of neutrino mass in oscillation experiments [3] makes the search for the Majorana nature of neutrinos particularly relevant and timely. Kinematic measurements restrict the neutrino mass scale to be below 1 eV [4].

The neutrino mass $m_\nu$ is one of a set of parameters which have been used to calculate the half life time of the 0νββ decay mode $T^{0\nu}$ form the following expression:

$$T^{0\nu} = 1 / F^{0\nu} ( M^{0\nu} m_\nu )^2 \quad (1)$$

The probability of occurrence of the 0νββ decay mode $P^{0\nu}$ is defined as the ratio between the total half life time of a ββ decay $T^t$ and $T^{0\nu}$. Thus according to eqn. (1) $P^{0\nu}$ is given by

$$P^{0\nu} = K ( M^{0\nu} m_\nu )^2 \quad (2)$$

K is the product of $T^t$ and the phase space factor $F^{0\nu}$ of the 0νββ decay mode. Recently[5,6,7,8,], it has been reported that $T^t$ is determined experimentally by different techniques for some double beta decay emitters : $^{82}Se$ , $^{100}Mo$ , $^{116}Cd$ , $^{128}Te$ , $^{130}Te$ , $^{136}Xe$. Table (1) presents the values of $T^t$ , $F^{0\nu}$ , K for these emitters.

The parameter $M^{0\nu}$ is the nuclear matrix element of the 0νββ decay mode of an emitter. It consists of three main factors: (1) Gammow-Teller transition matrix element $(M_{GT})^{0\nu}$ of the 0νββ decay mode. (2) Fermi transition matrix element $(M_F)^{0\nu}$ of the same mode. (3) the ratio $g_\nu / g_A$ , where $g_\nu$ , $g_A$ are the vector , axial-vector nuclear currents. They are related to $M^{0\nu}$ by the following relation: $M^{0\nu} = (M_{GT})^{0\nu} - (g_\nu / g_A)^2 (M_F)^{0\nu}$

Table (1) $T^t$ , $F^{0\nu}$ , K for some double beta decay emitters

| Emitter | $T^t$ x$10^{24}$ (y) | $F^{0\nu}$x$10^{-25}$ ($y^{-1}eV^{-2}$) | K |
|---|---|---|---|
| $^{82}Se$ | 0.36 [5] | 1.05 [9] | 0.03780 |
| $^{100}Mo$ | 1.10 [5] | 4.33* [10] | 0.47630 |
| $^{116}Cd$ | 0.17 [5] | 1.79* [10] | 0.03043 |
| $^{128}Te$ | 1.50 [6] | 0.0636 [9] | 0.00954 |
| $^{130}Te$ | 2.80 [7] | 1.59 [9] | 0.44520 |
| $^{136}Xe$ | 5.70 [8] | 1.67 [9] | 0.95190 |

*These are the values reported in Ref.[10] divided by $(m_e)^2$.($m_e = 0.511$x $10^6$ eV)

Previously [10], the variation of $M^{0\nu}$ with the strength of the particle- particle interaction $g_{pp}$ has been shown graphically [see Fig. (1)] by using pn-QRPA , pn-RQRPA , full-RQRPA , SQRPA techniques with small and large basis of the Hilbert space. The proton-neutron quasi particle random phase approximation (pn-QRPA) have clarified that the particle-particle interaction, which is the counterpart of the particle-hole interaction, enhances the spin-isospin correlations in the ground-state wave functions. The SQRPA technique uses the boson expansion for the phonon and β operators associated with pn-QRPA technique [11]. An alternative approach for extending pn-QRPA is based on the idea of partial restoration of the Pauli exclusion principle by taking into account the next terms in the commutator of the like nucleon operator involved in the derivation of the pn-QRPA equations [10]. The commutator is replaced by its expectation value in the RPA (correlated) g.s and this leads to a renormalization of the relevant operators and of the forward and backward going QRPA amplitudes as

well. This technique is called pn-RQRPA. It has been extensively used for both 2νββ and 0νββ decay modes and for transition to g.s. and excited states and for different nuclei [12,13]. The extension of this technique when the proton-neutron pairing interactions, besides the proton-proton and neutron-neutron ones, are also included was called the full-RQRPA [14].

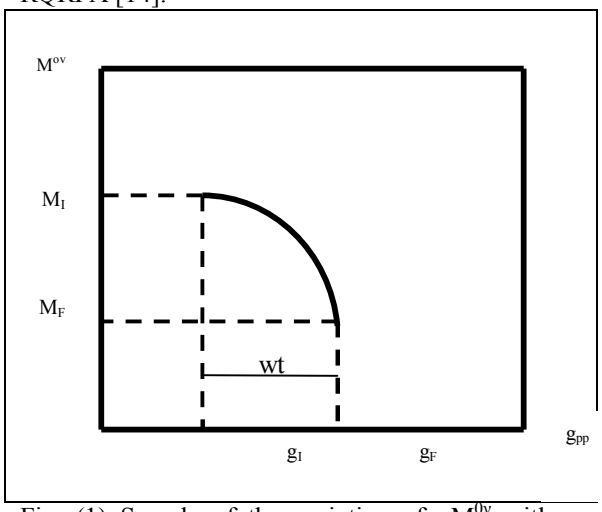


Fig. (1) Sample of the variation of $M^{0v}$ with $g_{pp}$ within the range $g_I \leq g_{pp} \leq g_F$. It has been reported that [10]: $g_I = 0.8$ and $g_F = 1.3$ for SQRPA technique and: $g_I = 0.8$ and $g_F = 1.4$ for pn-QRPA , pn-RQRPA , full-RQRPA techniques.

This work presents a procedure to determine the neutrino mass as well as : (1) theoretical calculation of $M^{0v}$ obtained by different nuclear models.
(2) experimental determinations of $F^{0v}$ and $T^t$ [see table (1)] collected from different laboratories.

**Distribution of $P^{0v}$ with $g_{pp}$**

According to eqn.(2), it is expected that the distribution of $P^{0v}$ with $g_{pp}$ is similar to that shown in fig.(1) such that $m_v$ is constant. Fig.(2) presents a sample of the expected variation of $P^{0v}$ with $g_{pp}$ in which a set of distributions A , B , C , D , E are presented.
Although the distributions shown in fig. (2) have similar behaviour to that shown in fig.(1) however they have different properties :
Curve A :
For all points on this curve the 0νββ decay mode is allowed ($P^{0v} \leq 100$ %) and less probable than the other decay mode (2νββ decay mode) ($P^{0v} < 50$ % ).

Curve B :
For all points on this curve the 0νββ decay mode is allowed ($P^{0v} \leq 100$ %) . This decay mode is less probable than the 2νββ decay mode ($P^{0v} < 50$ % ) for some points and more allowed than the 2νββ decay mode ($P^{0v} > 50$ % ) for the remaining points.
Curve C :
For all points on this curve the 0νββ decay mode is allowed ($P^{0v} \leq 100$ %) and more probable than the 2νββ decay mode ($P^{0v} > 50$ % ).

Curve D :
The 0νββ decay mode is allowed ($P^{0v} \leq 100$ %) and more probable than the 2νββ decay mode ($P^{0v} > 50$ %) for some points on this curve and not allowed ($P^{0v} > 100$ %) for the remaining points.
Curve E :
For all points on this curve the 0νββ decay mode is not allowed ($P^{0v} > 100$ %) .
The above properties are summarized in table (2)

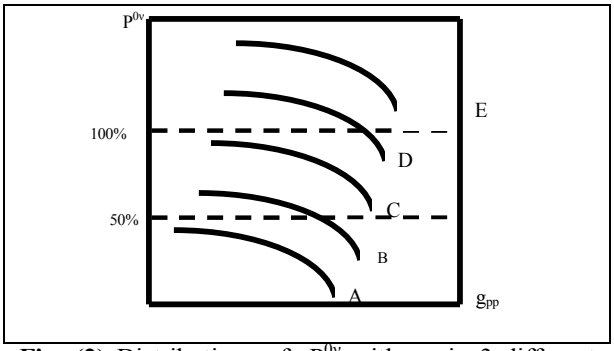


**Fig. (2)** Distributions of $P^{0v}$ with $g_{pp}$ in 3 different regions: (1) less probable ($0<P^{0v} < 50\%$) (2) more probable ($100\% > P^{0v} > 50\%$) (3) forbidden region ($P^{0v} > 100\%$)

**Table(2)** Properties of the distributions shown in fig. (2)

| Curve | Allowed | not allowed | Less probable | more probable |
|---|---|---|---|---|
| A | All | ___ | All | ___ |
| B | All | ___ | Some | Some |
| C | All | ___ | ___ | All |
| D | Some | Some | ___ | All |
| E | ___ | All | ___ | All |

It is clear that curve C is the best one in fig.(2) and table (2).

**Operating region**

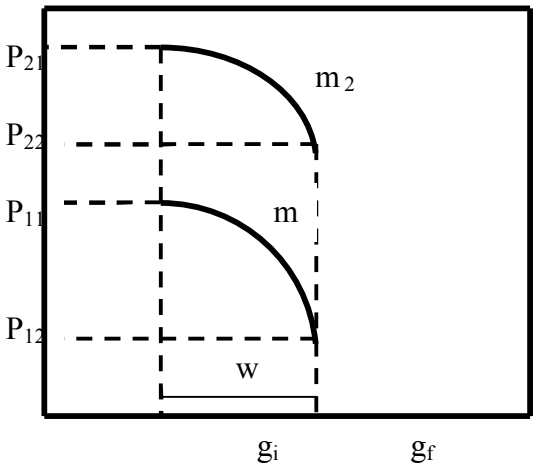


Fig. (3) Operating region parameters: (1) the lower and upper neutrino mass limits $m_1$, $m_2$ (2) the horizontal boundaries $g_i$, $g_f$ (3) the vertical boundaries $P_{11}$, $P_{21}$ $P_{22}$ , $P_{12}$

A set of distributions of $P^{0\nu}$ with $g_{pp}$ construct an operating region as shown in fig. (3). According to eqn. (2), the lowest and highest distributions shown in fig. (3) correspond to the lower and upper neutrino mass limits $m_1$ , $m_2$ . The horizontal coordinates of the operating region boundaries are $g_i$ , $g_f$ . R is defined as the ratio between the operating region width w [see fig. (3)] and the total available width $W_t$ of $g_{pp}$ [see fig. (2)]. Using the data in fig. (1) it is possible to express R as follows :

$R = w / 0.5$ for SQRPA technique (3)

$R = w / 0.6$ for pn-QRPA , pn-RQRPA , full-RQRPA techniques (4)

According to eqn. (2), the vertical coordinates $P_{11}$, $P_{21}$ $P_{22}$ , $P_{12}$ of the operating region boundaries [see fig.(2) and fig. (3)] are given by :

$P_{21} = K (M_i m_2)^2$ (5)

$P_{22} = K (M_f m_2)^2$ (6)

$P_{11} = K (M_i m_1)^2$ (7)

$P_{12} = K (M_f m_1)^2$ (8)

In the above eqns. $M_i$ and $M_f$ are the nuclear matrix elements which correspond to $g_i$ , $g_f$ . It can be summarized that the operating region parameters are: $m_1$ , $m_2$ , $g_i$ , $g_f$ , R , $P_{11}$, $P_{21}$ $P_{22}$ , $P_{12}$ .

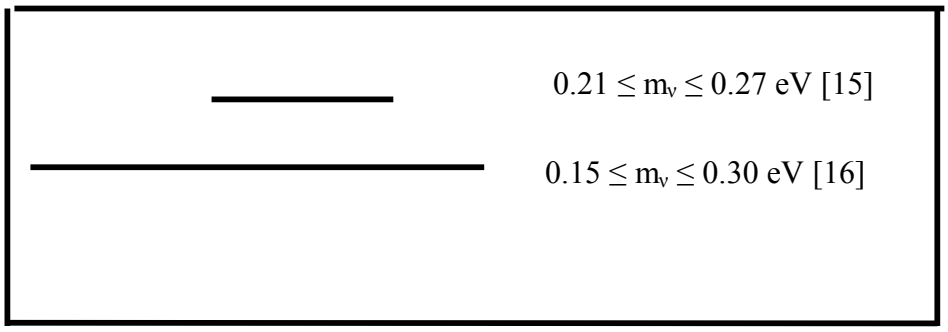


Fig. (4) Different values of $m_1 \leq m_\nu \leq m_2$ obtained from different sources

**Determination of the operating region parameters**

**(1) $m_1$ , $m_2$**

Fig. (4) presents the range $m_1 \leq m_\nu \leq m_2$ obtained from different laboratories [15,16].

The lower and upper neutrino mass limits $m_1$, $m_2$ are related to the neutrino mass $m_\nu$ and its uncertainty $\delta m_\nu$ by the following relations:

$m_\nu = (m_2 + m_1) / 2$ (9)

$\delta m_\nu = (m_2 - m_1) /2$ (10)

According to eqns. (9) , (10) the values of $m_1$ , $m_2$ shown in fig.(4) correspond to neutrino mass $m_\nu$ and its uncertainty $\delta m_\nu$ which are given by :

$m_\nu \pm \delta m_\nu = 0.240 \pm 0.030$ eV [15] (11)

$m_\nu \pm \delta m_\nu = 0.225 \pm 0.075$ (12)

The relative uncertainties of eqns. (11) ,(12) are $\delta m_\nu / m_\nu$=12.5 % and 33.33 % respectively. To improve these values, $\delta m_\nu / m_\nu$ is selected in this work to be 8 %. According to eqns. (9), (10) this choice produces the following relations:

$m_1 = 0.852\, m_2$ (13)

$m_\nu \pm \delta m_\nu = 0.926\, m_2 \pm 0.074\, m_2$ (14)

**(2) $P_{11}$, $P_{21}$ $P_{22}$ , $P_{12}$**

Eqn. (13) is used in eqns. (5) , (6) , (7) , (8) to get the following relations :

$P_{11} / P_{21} = P_{12} / P_{22} = 0.7259$ (15)

**(3) $g_i$, $g_f$ , R**

In this work $g_i$ [ see fig. (3)] = $g_I$ [ see fig. (2) ] = 0.8. Determination of $g_f$ , w , R depend on the choice of the parameter $P_{12}$ or $P_{22}$ as shown in fig. (3).

## 3. Results and discussion

The upper value $P_{21}$ of the vertical boundaries of the operating region is selected to be the maximum allowed value of $P^{0\nu}$ which is 100%. The values of K listed in table (1) for $^{82}Se$ , $^{100}Mo$ , $^{116}Cd$ , $^{128}Te$ , $^{130}Te$ , $^{136}Xe$ have been used with the known values of $M_i$ obtained from pn-QRPA , pn-RQRPA , full-RQRPA and SQRPA techniques with small and large basis of Hilbert space [10] to calculate $m_2$, $m_1$ from eqns.(5), (13).. The results of calculations are classified into 3 sets:

Set (1): the range $m_1 \leq m_\nu \leq m_2$ agrees with fig. (4) [see table (3)].

Set (2): the range $m_1 \leq m_\nu \leq m_2$ disagrees with fig. (4) and close to it [see table(4)].

Set (3): the range $m_1 \leq m_\nu \leq m_2$ disagrees with fig. (4) and far from it [see table(5)].

Table (3) Upper and lower neutrino mass limits which are consistent with fig. (4)

| Pn-QRPA | | Pn-RQRPA | | Full-RQRPA | | SQRPA | | |
|---|---|---|---|---|---|---|---|---|
| S | L | S | L | S | L | S | L | Element |
| 0.264 0.225 | _____ | 0.309 0.263 | 0.299 0.255 | 0.299 0.255 | _____ | _____ | _____ | $^{100}Mo$ |
| 0.313 0.267 | _____ | 0.291 0.248 | _____ | 0.281 0.239 | _____ | _____ | _____ | $^{130}Te$ |
| _____ | _____ | _____ | _____ | _____ | _____ | 0.248 0.211 | 0.263 0.224 | $^{136}Xe$ |

Table (4) Upper and lower neutrino mass limits which disagree with the range shown fig.(4) and close to it

| Pn-QRPA | | Pn-RQRPA | | Full-RQRPA | | SQRPA | | |
|---|---|---|---|---|---|---|---|---|
| S | L | S | L | S | L | S | L | Element |
| _____ | 0.376 0.320 | _____ | _____ | _____ | 0.362 0.308 | 0.356 0.303 | 0.377 0.321 | $^{100}Mo$ |
| _____ | 0.361 0.307 | _____ | 0.393 0.335 | _____ | 0.375 0.319 | _____ | _____ | $^{130}Te$ |

Table (5) Upper and lower neutrino mass limits which disagree with the range shown in fig.(4) and far from it

| Pn-QRPA | | Pn-RQRPA | | Full-RQRPA | | SQRPA | | |
|---|---|---|---|---|---|---|---|---|
| S | L | S | L | S | L | S | L | Element |
| 0.902 0.768 | 1.09 0.929 | 1.19 1.014 | 1.648 1.404 | 1.123 0.957 | 1.775 1.512 | 1.225 1.044 | 1.429 1.217 | $^{82}Se$ |
| 1.478 1.259 | 1.887 1.608 | 1.309 1.115 | 1.727 1.471 | 1.964 1.673 | 2.249 1.916 | 1.215 1.035 | 1.236 1.053 | $^{116}Cd$ |
| 1.819 1.550 | 2.402 2.046 | 1.907 1.625 | 2.63 2.240 | 1.822 1.552 | 2.449 2.086 | 3.141 2.676 | 3.386 2.885 | $^{128}Te$ |
| _____ | _____ | _____ | _____ | _____ | _____ | 0.629 0.536 | 0.771 0.657 | $^{130}Te$ |
| 0.484 0.412 | 0.59 0.503 | 0.457 0.389 | 0.498 0.424 | 0.446 0.38 | 0.554 0.472 | _____ | _____ | $^{136}Xe$ |

The following sections present the values of $P_{21}$, $P_{12}$ of the operating regions [see fig. (3)] for the 3 sets which are selected to make agreement between the values of neutrino mass for all the emitters used in this work and fig. (4).

### Operating region parameters of SET (1)

In this set the vertical boundaries of the operating region [see fig. (3)] are selected such that: (1) the largest probability in this region $P_{21}$ is the maximum allowed value for $P^{0\nu}$ which is 100%. (2) The lower boundary $P_{12}$ is selected to be 50% .to get the largest possible width of $g_{pp}$ such that the whole operating region is similar to curve C (the best curve in fig.(2) and table (2)]. Using eqns. (12),(13) the vertical boundaries of set (1) are:

$P_{21}$ = 100%, $P_{11}$ = 72.59%, $P_{22}$ = 68.88%, $P_{12}$ = 50%

The values of $m_2$ listed in table (3) have been used to calculate new values of $m_\nu \pm \delta m_\nu$ from eqn. (14) and the results are presented in table (6). In this table the best value of $m_\nu \pm \delta m_\nu$ is 0.269 ± 0.0216 eV which has the largest value of R = 61.7%. It belongs to $^{130}Te$ and pn-RQRPA technique with small basis.

Table (6) Operating region parameters for set (1): $m_\nu \pm \delta m_\nu$ (eV) , $g_i$ , $g_f$ ,R%

| $^{100}Mo$ | | | | |
|---|---|---|---|---|
| Technique | Basis | $m_\nu \pm \delta m_\nu$ (eV) | $g_i \leq g_{pp} \leq g_f$ | R% |
| Pn-QRPA | Small | 0.244 ± 0.020 | $0.8 \leq g_{pp} \leq 1.115$ | 52.5 |
| Pn-RQRPA | Small | 0.286 ± 0.023 | $0.8 \leq g_{pp} \leq 1.070$ | 45.0 |
| Pn-RQRPA | Large | 0.277 ± 0.022 | $0.8 \leq g_{pp} \leq 1.100$ | 50.0 |
| Full-RQRPA | Small | 0.277 ± 0.022 | $0.8 \leq g_{pp} \leq 1.093$ | 48.8 |
| $^{130}Te$ | | | | |
| Pn-QRPA | Small | 0.290± 0.023 | $0.8 \leq g_{pp} \leq 1.066$ | 44.3 |
| Pn-RQRPA | Small | 0.269 ± 0.0216 | $0.8 \leq g_{pp} \leq 1.170$ | 61.7 |
| Full-RQRPA | Small | 0.260 ± 0.0213 | $0.8 \leq g_{pp} \leq 1.100$ | 50.0 |
| $^{136}Xe$ | | | | |
| SQRPA | Small | 0.230 ± 0.0180 | $0.8 \leq g_{pp} \leq 0.950$ | 30.0 |
| SQRPA | Large | 0.243 ± 0.0198 | $0.8 \leq g_{pp} \leq 0.940$ | 28.0 |

### Operating region parameters of SET (2)

To make a consistency between the results of table (4) and fig.(4) $P_{21}$ should be <100% . The values of $P_{21}$ listed in table (7) are selected such that

the lower limit ($m_v$ - $\delta m_v$) is very close to the upper limit 0.3 eV of the range shown in fig. (4). The lower boundary $P_{12}$ is selected to be 50% like set (1). The operating region of set (2) is similar to curve C in fig. (2) [see table (2)]. The best value of $P_{21}$ is 95% which belongs to $^{100}$Mo and SQRPA technique with small basis. On the other hand the best value of R is 35% which belongs to $^{100}$Mo and pn-QRPA technique with large basis. Therefore a compromise has to be done between $P_{21}$ and R to select the best result of set (2).

**Table (7)** Operating region parameters for set (2): $P_{21}$ , $m_v$ $\pm$ $\delta m_v$ (eV) , $g_i$ , $g_f$ ,R%

| $^{100}$Mo | | | | | |
|---|---|---|---|---|---|
| Technique | Basis | $P_{21}$% | $m_v \pm \delta m_v$(eV) | range of $g_{pp}$ | R% |
| pn-QRPA | Large | 85 | 0.321±0.024 | $0.8 \le g_{pp} \le 1.01$ | 35 |
| full-RQRPA | Large | 90 | 0.318±0.024 | $0.8 \le g_{pp} \le 0.99$ | 32 |
| SQRPA | Small | 95 | 0.321±0.024 | $0.8 \le g_{pp} \le 0.90$ | 20 |
| SQRPA | Large | 85 | 0.322±0.024 | $0.8 \le g_{pp} \le 0.86$ | 11 |
| $^{130}$Te | | | | | |
| pn-QRPA | Large | 90 | 0.317±0.023 | $0.8 \le g_{pp} \le 0.93$ | 21 |
| Pn-RQRPA | Large | 75 | 0.315±0.025 | $0.8 \le g_{pp} \le 0.98$ | 29.6 |
| full-RQRPA | Large | 85 | 0.320±0.024 | $0.8 \le g_{pp} \le 1.00$ | 34 |

**Operating region parameters of SET (3)**

The situation in set (3) is different from that in sets (1) and (2). The upper boundary $P_{21}$ has to be greatly reduced to attain consistency between the results of table (5) and fig. (4). The values of $P_{21}$ listed in table (8) are selected such that the lower limit $m_1$ equals to the upper limit 0.3 eV of the range shown in fig. (4).These values are the maximum allowed values of $P^{0\nu}$ for the members of set (3) to make an agreement with fig. (4). This means that the ($0\nu\beta\beta$) decay mode takes place in set (3) with poor probability. The lower boundary $P_{12}$ is selected such that the operating region width w is half the total available width $W_t$ . The majority of the distributions in the operating region of set (3) are similar to curve A in fig.(2) while the other distributions are the same as curve B. The neutrino mass $m_v \pm \delta m_v$ and the ratio R for set (3) are given by :

$m_v \pm \delta m_v = 0.326 \pm 0.026$ eV, R = 50%

**Recommendations**

There are some recommendations for the emitters used in this work:

(I) $^{100}$Mo, $^{130}$Te, $^{136}$Xe:

The techniques used successfully with these emitters to give acceptable results for neutrino mass are listed in tables (6) and (7).

(II) $^{82}$Se, $^{116}$Cd, $^{128}$Te:

The values of neutrino mass of the emitters $^{82}$Se, $^{116}$Cd, $^{128}$Te which are listed in table (5) should be reduced by a factors of about 6.5, 9,13 respectively to make consistency with fig. (4). According to eqn. (2) this reduction corresponds to 3 different cases:

**Table (8)** Operating region parameters for set (3): $P_{21}$, $P_{11}$ , $P_{12}$ , $P_{22}$

| $^{82}$Se | | | | | |
|---|---|---|---|---|---|
| Technique | Basis | $_{21}$% | $P_{11}$% | $P_{12}$% | $P_{22}$% |
| pn-QRPA | Small | 15.24 | 11.06 | 8.38 | 11.55 |
| pn-QRPA | Large | 10.44 | 7.58 | 5.37 | 7.4 |
| pn-RQRPA | Small | 8.76 | 6.36 | 4.85 | 6.68 |
| pn-RQRPA | Large | 4.56 | 3.31 | 1.4 | 1.93 |
| full-RQRPA | Small | 9.83 | 7.14 | 5.16 | 7.11 |
| full-RQRPA | Large | 3.93 | 2.86 | 2.16 | 2.98 |
| SQRPA | Small | 8.26 | 6.0 | 4.55 | 4.75 |
| SQRPA | Large | 6.07 | 4.4 | 2.41 | 3.32 |
| $^{116}$Cd | | | | | |
| Technique | Basis | $P_{21}$% | $P_{11}$% | $P_{12}$% | $P_{22}$% |
| pn-QRPA | Small | 5.68 | 4.12 | 3.29 | 4.53 |
| pn-QRPA | Large | 3.48 | 2.53 | 1.215 | 1.67 |
| pn-RQRPA | Small | 7.23 | 5.25 | 2.795 | 3.85 |
| pn-RQRPA | Large | 4.15 | 3.02 | 1.89 | 2.6 |
| full-RQRPA | Small | 3.21 | 2.33 | 1.68 | 2.31 |
| full-RQRPA | Large | 2.45 | 1.78 | 1.28 | 1.76 |
| SQRPA | Small | 8.40 | 6.10 | 2.87 | 3.96 |
| SQRPA | Large | 8.12 | 5.89 | 2.25 | 3.09 |
| $^{128}$Te | | | | | |
| Technique | Basis | $P_{21}$% | $P_{11}$% | $P_{12}$% | $P_{22}$% |
| pn-QRPA | Small | 3.75 | 2.72 | 1.14 | 1.57 |
| pn-QRPA | Large | 2.15 | 1.63 | 0.43 | 0.59 |
| pn-RQRPA | Small | 3.41 | 2.47 | 1.95 | 2.19 |
| pn-RQRPA | Large | 1.79 | 1.30 | 0.89 | 1.23 |
| full-RQRPA | Small | 3.74 | 2.71 | 1.73 | 2.38 |
| full-RQRPA | Large | 2.07 | 1.50 | 1.097 | 1.51 |
| SQRPA | Small | 1.26 | 0.91 | 0.496 | 0.68 |
| SQRPA | Large | 1.08 | 0.78 | 0.355 | 0.49 |
| $^{130}$Te | | | | | |
| Technique | Basis | $P_{21}$% | $P_{11}$% | $P_{12}$% | $P_{22}$% |
| SQRPA | Small | 31.34 | 22.75 | 5.01 | 6.9 |
| SQRPA | Large | 20.86 | 15.14 | 5.86 | 8.07 |
| $^{136}$Xe | | | | | |
| Technique | Basis | $P_{21}$% | $P_{11}$% | $P_{12}$% | $P_{22}$% |
| pn-QRPA | Small | 52.93 | 38.42 | 15.24 | 21.0 |
| pn-QRPA | Large | 35.62 | 25.86 | 6.01 | 8.28 |
| pn-RQRPA | Small | 59.43 | 43.14 | 17.12 | 23.58 |
| pn-RQRPA | Large | 49.9 | 36.22 | 11.54 | 15.9 |
| full-RQRPA | Small | 62.42 | 45.31 | 16.49 | 22.72 |
| full-RQRPA | Large | 40.4 | 29.33 | 10.82 | 14.91 |

**Case (1):**

In this case $T^t$, $M^{0\nu}$, $P^{0\nu}$ are kept without change and the values of $F^{0\nu}$ listed in table (1) are multiplied by a factors of about 40, 80,170. This corresponds to multiply the Q-values of these emitters by another factors: 2.1, 2.4,2.8 because $F^{0\nu}$ is approximately proportional to $Q^5$ [17]. It is not possible to verify this case because the Q-values of the emitters $^{82}$Se, $^{116}$Cd, $^{128}$Te are well determined by the Atomic Mass Evaluation [18].

**Case (2):**

In such case $F^{0v}$, $M^{0v}$, $P^{0v}$ are kept constant. The values of $T^t$ listed in table (1) should be multiplied approximately by 40, 80, 170 to be 14.5 x $10^{24}$ y , 13.5 x $10^{24}$ y , 255 x $10^{24}$ y for the emitters $^{82}$Se, $^{116}$Cd, $^{128}$Te respectively.

**Case (3):**

In this case $T^t$, $F^{0v}$, $P^{0v}$ are kept constant while the values of $M^{0v}$ of the emitters $^{82}$Se, $^{116}$Cd, $^{128}$Te [10] are multiplied by a factors of about 6.5,9,13 respectively. Such multiplication produces a new values of $M^{0v}$ which are far from the normal range determined by many groups [10,19,20,21,22,23,24,25]. Therefore this case is not acceptable.

Case (2) is the best candidate from the above 3 cases. So this work recommends to remeasure $T^t$ of $^{82}$Se, $^{116}$Cd, $^{128}$Te to be approximately 14.5 x $10^{24}$ y , 13.5 x $10^{24}$ y , 255 x $10^{24}$ y to make consistency with previous determinations shown in fig. (4).

**Conclusion**

The probability of occurrence of the 0νββ decay mode $P^{0v}$ depends on the neutrino mass $m_v$ and the strength of the particle- particle interaction $g_{pp}$ The variation of $P^{0v}$ with $g_{pp}$ is presented graphically within a certain width $W_t$ of $g_{pp}$ such that $m_v$ is kept constant on the graph. An operating region is a region bounded by the lower and upper limits of $P^{0v}$ and $m_v$ . The width of $g_{pp}$ for this region is w and can be expressed as ratio R = w / $W_t$. The limits of an operating region are calculated for 6 double beta decay emitters : $^{82}$Se , $^{100}$Mo , $^{116}$Cd , $^{128}$Te , $^{130}$Te , $^{136}$Xe by using pn-QRPA , pn-RQRPA , full-RQRPA and SQRPA techniques with small and large basis of Hilbert space. This procedure produces 48 operating regions such that the relative uncertainty $\delta m_v / m_v$ of each region is 8% which improves the previous determination 12.5%. These regions are divided into 3 sets. The first set contains 9 regions in which $P^{0v}$ varies between 50% and 100% and R varies between 28% and 61.7%. In the second set $P^{0v}$ varies between 50% and 95 % and R varies between 11% and 35% for 7 regions. The third set contains 32 operating regions in which $P^{0v}$ varies between 0.355% and 62.42 while R=50%. Set (3) has a poor probability in comparison with sets (1) and (2). In this work the best operating region exists in set (1) and belongs to $^{130}$Te and pn-RQRPA technique with small basis of Hilbert space. In this region $m_v \pm \delta m_v$ is 0.269 ± 0.0216 eV and R=61.7%.

Corresponding author
**M. H. Sidky**
Department of Engineering, Mathematics and Physics, Faculty of Engineering, Cairo University, Egypt
sidkym@yahoo.com

**References**

[1] Schechter J. and J.W.F.Valle, Phys. Rev. D 25 (1982) 2951
[3] Nakamura K. et al. (Particle Data Group) J. Phys.G 37 (2010) 075021.
[4] Aseev V.N. *et al.* Phys. Rev. D 84 (2011) 112003
Kraus Ch. *et al* . , Eur. Phys. J. C40 (2005) 447.
[5] Barabash A.S., …..Phys. of Particles and Nuclei , Vol 42 , No. 4, (2011) 613.
[6] Barabash A.S., ….Phys. Rev. C81, (2010) .
[7] Andreotti E. *et al.*Astrop. Phys. 34 (2011) 822.
[8] Kamland-Zen Collabration Phys. Rev. C85, (2012) 045504.
[9] Suhonen J. Nucl. Phys. A 847 (2010) 207.
[10] Stoica S. *et al.* Nucl. Phys. A 694 (2001) 269.
[11] Raduta A A *et al.* Nucl. Phys. A 534 (1991) 149.
[12] Schwieger J. *et al.* Phys. Rev. C57 (1998)1738.
[13 ]Suhonen J. and O.Civitarese Phys. Rep. 300, (1998) 123.
[14] Simovic F. *et al.* Phys. Lett. 393 (1997)267
[15] Faessler A. , Journal of Physics Conference Series 267 (2011) 012059.
[16] EJiri H. , Journal of Physical Society of Japan , Vol 74 , No. 8, (Aug. 2005) 2101.
[17] Moe M. and P.Vogel , Ann. Rev. Nucl. Part. Sci., 44 (1994) 254.
[18] Wapstra A.H. *et al.* Nucl. Phys. A 729 (2003) 129-336.
[19] Haxton W.C. and G.J.Stephenson Jr., Prog. Part. Nucl. Phys. 12 (1984) 409.
[20] Vogel P. and M.R. Zirnbauer Phys. Rev. Lett. 57 (1986)3148.
[21] Civitarese O. *et al.* Phys. Lett. B194 (1987)11.
[22] Tomoda T. and Amand Faessler , Phys. Lett. B199 , No. 4 (1987) 475.
[23] Engel J. *et al.* Phys. Lett. B225, No. 1,2 (1989)5.
[24] Muto K. *et al.* Z. Phys A334 (1989)187.
[25] Benes P. *et al.*, Acta Physica Polonica B37 (2006)1927.

12/25/2012